Icarus 206 (2010) 345–351

Contents lists available at ScienceDirect

Icarus

journal homepage: www.elsevier.com/locate/icarus

Ground-based measurements of the methane distribution on Titan

Paulo F. Penteado *, Caitlin A. Griffith

Department of Planetary Sciences, The University of Arizona, Tucson, AZ 85721, USA

ARTICLE INFO

Article history:
Received 24 April 2009
Revised 27 August 2009
Accepted 31 August 2009
Available online 6 September 2009

Keywords:
Titan
Satellites, Atmospheres
Abundances, Atmospheres
Spectroscopy
Radiative transfer

ABSTRACT

Using spectra taken with NIRSPEC (Near Infrared Spectrometer) and adaptive optics on the Keck II telescope, we resolved the latitudinal variation of the $3\nu_2$ band of CH_3D at 1.56 μm. As CH_3D is less abundant than CH_4 by a factor of $50 \pm 10 \times 10^{-5}$, these CH_3D lines do not saturate in Titan's atmosphere, and are well characterized by laboratory measurements. Thus they do not suffer from the large uncertainties of the CH_4 lines that are weak enough to be unsaturated in Titan. Our measurements of the methane abundance are confined to the latitude range of 32°S–18°N and longitudes sampled by a 0.04″ slit centered at ~195°W. The methane abundance below 10 km is constant to within 20% in the tropical atmosphere sampled by our observations, consistent with the low surface insolation and lack of surface methane [Griffith, C.A., McKay, C.P., Ferri, F., 2008. Astrophys. J. 687, L41–L44].

1. Introduction

In Titan's lower atmosphere, methane cycles between gaseous and condensed forms. Measurements of the global methane abundance and distribution of clouds and surface fluvial features, coupled with theoretical studies, partially constrain the methane cycle. Yet, a determination of the spatial distribution of atmospheric methane is still lacking.

Tropospheric clouds were identified from Titan's ground-based spectra recorded in 1995 (Griffith et al., 1998, 2000). The first images of clouds in 2000 (Roe et al., 2002; Brown et al., 2002) revealed that they resided near the south pole. In 2004, ground-based observations displayed a band of clouds near 40°S latitude (Roe et al., 2005a), which, along with the polar clouds, have been subsequently observed and studied with Cassini and ground-based data (Porco et al., 2005; Griffith et al., 2005; Brown et al., 2006; Roe et al., 2005b; Schaller et al., 2006a; Gendron et al., 2004; Gibbard et al., 2004; Hirtzig et al., 2005; Bouchez and Brown, 2005), though the polar clouds have become less frequent since 2004 (Schaller et al., 2006b). More recently, methane clouds have appeared at tropical latitudes (Griffith et al., 2009; Schaller et al., 2009), and at high northern latitudes (Brown et al., 2009). Similar to Earth's convective clouds, Titan's methane clouds evolve in timescales of hours (Griffith et al., 2000), and can reach the tropopause, where they are spread by zonal winds (Griffith et al., 2005).

The latitudinal distribution of southern hemisphere clouds correlates with that of updrafts in the general circulation, indicating that mechanical forcing is involved in cloud formation (Rannou et al., 2006; Mitchell et al., 2006). The northern methane clouds appear, instead, at latitudes containing the north polar lakes (Brown et al., 2009), suggesting that unstable conditions also result from a rise in humidity through evaporation. Cassini RADAR observations indicate that larger and deeper channels concentrate at middle and high latitudes, indicating a greater occurrence of rainfall (Lorenz et al., 2008). Clouds have also appeared near the southern lake Ontario Lacus (Schaller et al., 2006a; Brown et al., 2008), where the appearance of dark features after the clouds passed indicated the advent of rainfall (Turtle et al., 2009). In Titan's tropics, the low surface humidity of 45% renders the atmosphere highly stable (Barth and Rafkin, 2007; Griffith et al., 2008). Unlike the polar conditions, tropical seasonal variations in the insolation are likely too weak to power sufficient evaporation to significantly change the humidity (Griffith et al., 2008). In addition, there is no evidence for liquid methane surfaces at latitudes between 50°N and 50°S (Stofan et al., 2007). Thus a uniform and unchanging methane abundance has been predicted, along with clouds that, if convective, remain below 26 km altitude (Griffith et al., 2008). So far, such low convective clouds are consistent with observations (Griffith et al., 2009). The formation of the high clouds near the 40°S latitude band is also somewhat puzzling, because they reach the tropopause and display convective morphologies, thereby indicating convection of humid surface air (Griffith et al., 2005, 2008). Yet the underlying surface appears devoid of surface liquids.

* Corresponding author. Address: Universidade de São Paulo, IAG, Rua do Matão, 1226, São Paulo, SP 05508-090, Brazil.
E-mail addresses: penteado@astro.iag.usp.br, pfpenteado@yahoo.com (P.F. Penteado).

0019-1035/$ - see front matter © 2009 Elsevier Inc. All rights reserved.
doi:10.1016/j.icarus.2009.08.022

These clouds have been speculated to form from volcanic outgassing (Roe et al., 2005b) or circulation updrafts (Griffith et al., 2005, 2006).

Cryovolcanism is expected within the past 20 myr to supply the current 5 m of atmospheric methane, which is continually depleted by UV photolysis (Yung et al., 1984; Tobie et al., 2006). While this hypothesis is consistent with the rarity of craters, current cryovolcanic candidates do not correlate with observed cloud locations (Barnes et al., 2005; Sotin et al., 2005; Lopes et al., 2007).

Clouds in Titan's atmosphere thus suggest that variations in the humidity destabilize the lower troposphere, particularly at high latitudes. Yet, aside from the Huygens GCMS measurement of the methane vertical distribution at the probe site (Niemann et al., 2005; Tokano et al., 2006), and estimates from infrared Voyager observations (Samuelson et al., 1997), measurements have been limited to global average values, which range from 0.4 to 5.5 km-am (de Bergh et al., 1988; Lellouch et al., 1989, 1992; Courtin et al., 1995; Lemmon et al., 2002; Penteado et al., 2005). Recent observations of the 0.61 μm band by Cassini's Visual and Infrared Mapping Spectrometer (VIMS) determine the methane variations in the upper troposphere (20–50 km), but not the lower troposphere due to the low spectral resolution (Penteado et al., this issue). Here, we present and analyze high spectral resolution Keck data, which probe the methane near the surface.

2. Observations

Observations were recorded on December 18 2006 over a 2.5 h period centered at 15:05 UTC, with the Near Infrared Spectrometer (NIRSPEC, McLean et al., 1998) on the Keck II telescope.[1] The spectra, taken in échelle mode, cover the 1.46–1.64 μm region at resolution $R \sim 27{,}000$, sampled on 16 overlapping sections of 1024 pixels each. With the use of adaptive optics, the spatial resolution along the slit was 0.04″, sampled with 0.013″ pixels, which were binned in groups of 3 to attain 20 spatial resolution elements across Titan's disk. Fig. 1 shows a typical slit camera image, recorded with the NIRSPEC-5 filter (covering 1.46–1.64 μm), to indicate the location of the observations. The observing night was near Saturn's opposition, with a phase angle of 5.3°, and sub-observer point at 12.12°S, 196°E. At each grating setting, two spectra were obtained, with Titan on different positions along the slit, to subtract the sky contribution between the two nods. The borders of the disk were contaminated by light from the other image next to it, but these limb regions had to be discarded anyway due to their high emission angles with respect to Titan's surface. For the initial flux calibration we divided Titan's spectra by those of the nearby solar analogue G5 star, HD 85258, of H magnitude 5.758, which had a spatial FWHM of 0.035″. Titan's apparent full disk H magnitude was 7.9, but that of the portion falling on each pixel was only 16.3. The absolute flux calibration was further refined by matching the spectra of (Orton, 1992).

We determine the position of the slit on Titan's disk from the slit camera images, as the required precision is higher than the uncertainty in the telescope's pointing information. Titan's disk is an extended source, with brightness variations smaller than the contrast between the disk and background. Thus the surface of the disk has a relatively flat profile over an extended area, such that the disk center cannot be found by simply fitting a sharply peaked function as the instrument's point spread function. The slit camera images were filtered to remove noise and decrease the variations over Titan's disk. Wavelet transforms of the images with a radially symmetric kernel of the dimension of Titan's disk result in a function that is sharply peaked on the disk center, because here Titan's disk coincides with the positive part of the kernel. A least squares fit of a Gaussian surface to the wavelet transform then provides the coordinates for the center of the disk, which were averaged among all the slit camera images taken during each spectrum. The resulting coordinates for Titan's center have an uncertainty smaller than two sample pixels of size 0.013".

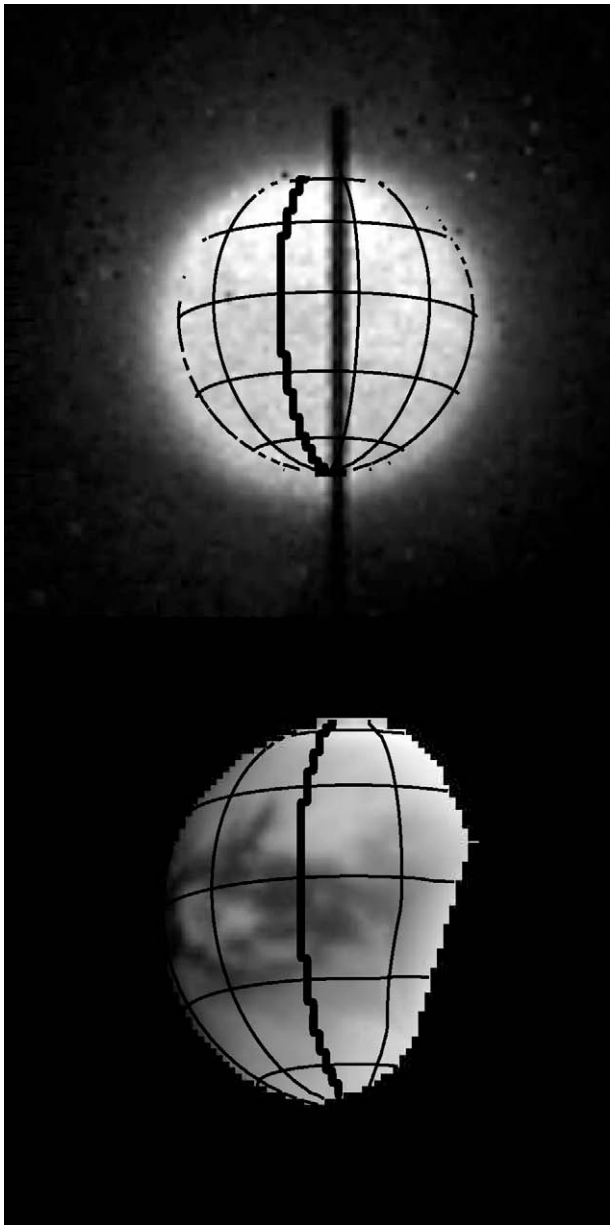

Fig. 1. Geometry reference images. Top: Average slit camera image at 1.46–1.64 μm. The lines are latitude and longitude contours, spaced at 30°, the thicker line is 180° longitude. Bottom: A VIMS 1.56 μm image, projected to the same geometry and similar pixel scale, indicating the location of the observations. The difference in contrast is due partly to the broader instrument PSF, and to the broader wavelength range of the NIRSPEC image, which includes wavelengths of high methane opacity around the 1.6 μm window.

Following Penteado et al. (2005), we analyzed lines from the $3\nu_2$ band of CH_3D that have well constrained absorption coefficients from laboratory measurements. The CH_3D lines are not saturated in Titan's atmosphere, as are the well measured CH_4 lines, and instead provide a sensitive measure of the abundance in the lowest 10 km of Titan's atmosphere. We chose a constant CH_3D/CH_4 ratio of $(50 \pm 10) \times 10^{-5}$, previously derived from unsaturated emission

[1] The data presented herein were obtained at the W.M. Keck Observatory, which is operated as a scientific partnership among the California Institute of Technology, the University of California and the National Aeronautics and Space Administration. The Observatory was made possible by the generous financial support of the W.M. Keck Foundation.

lines of CH_3D and CH_4 at 8.6 μm (Penteado et al., 2005), which is consistent with previous studies (de Bergh et al., 1988; Orton, 1992; Coustenis et al., 2003). However, as we derive relative variations in methane as a function of latitude, this choice does not affect our results. Fig. 2 displays the measured and calculated spectra. The effects of high incidence and emission angles render the interpretation unreliable at the five points nearest to the limb, that is, at latitudes 59°S, 51°S, 45°S, 25°N, 32°N. The methane abundance, as indicated by the weak CH_3D lines, can be inferred by comparing the observed and modeled spectra for several values of the surface relative humidity (Fig. 3); only at 1.5552–1.5562 μm is the CH_3D absorption comparable to that of CH_4.

3. Radiative transfer modeling of Titan's spectrum

To reproduce Titan's spectrum, we developed a radiative transfer model that incorporates the haze parameters and latitudinal variations derived from the Huygens DISR observations (Tomasko et al., 2008) and the analysis of Cassini VIMS observations at 0.4–1.6 μm (Penteado et al., this issue). The model approximates the radiative transfer solution using a discrete ordinates algorithm (DISORT, Stamnes et al., 1988) with 32 streams. The atmosphere was divided into 51 vertical homogeneous layers. We start with the methane vertical density profile measured by Huygens GCMS (Niemann et al., 2005). To fit the spectra, we either multiply the GCMS reference profile by a constant factor, or specify the methane vertical profile from its relative humidity at the surface. In the latter case, the mixing ratio is kept constant from the surface to the altitude where saturation is reached, from which 100% saturation is followed until the tropopause. The methane abundance thus is determined by a single parameter, the relative humidity at the surface, which is varied to fit the different spectra.

The CH_3D absorption was calculated with the coefficients measured in the laboratory by Boussin et al. (1999, 1998) and Lutz et al. (1983). The CH_4 absorption coefficients include corrections to the laboratory measurements, derived from Saturn spectra (de Bergh et al., 1988; de Bergh et al., 1986). As described by Tomasko et al. (2008) and Penteado et al. (this issue), the haze phase function was determined directly from the DISR observations, then fit to fractal particles. The haze optical depth is defined in three different regions: it decreases exponentially with a scaleheight of 65 km above 80 km, and increases linearly with decreasing altitude following different slopes within the regions 80–30 km and 30–0 km. Its wavelength variation is a power law, with different coefficients at each of these three altitude regions. The single scattering albedo also follows different functions for each of these three altitude regions, and is a linear interpolation in wavelength from the DISR measurements at 0.4–1.6 μm.

We interpret the data by matching it to calculated spectra at three wavelength regions (referred to as indicators), which are 1.55572–1.55607 μm for indicator i_0, 1.55517–1.55522 μm for

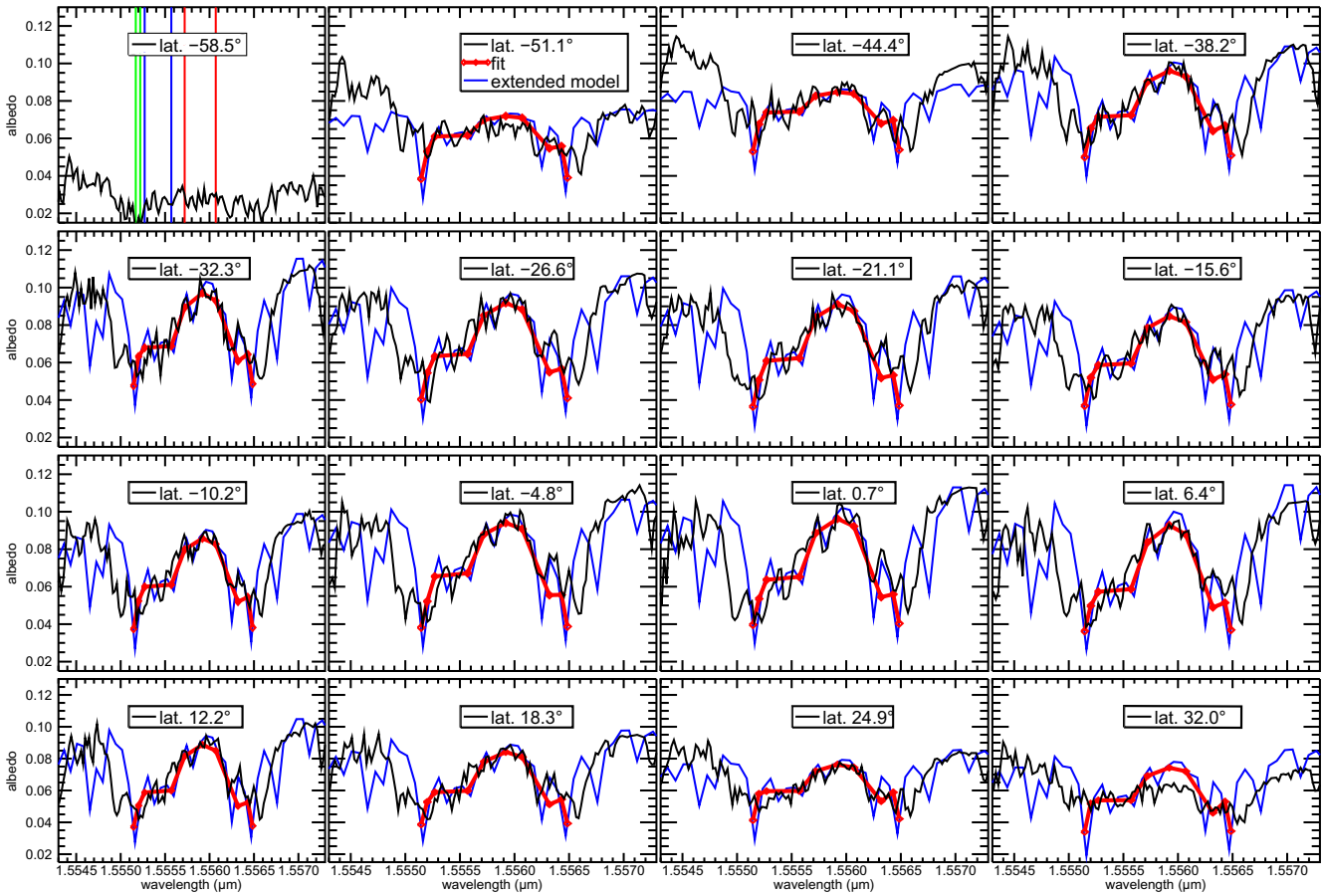

Fig. 2. The 16 measured spectra (black lines), along with the best model fits (red lines). The three southernmost and the two northernmost spectra are flattened by the higher opacity near the limb. This loss of the methane feature, along with the high variation in the lighting geometry within each pixel, makes the determinations of the model parameters unreliable at these locations. The vertical lines in the first spectrum indicate the wavelength ranges used to measure the three indicators: 1.55572–1.55607 μm for i_0 (red), 1.55517–1.55522 μm for i_1 (green), and 1.55527–1.55557 μm for i_2 (blue). The blue lines are models calculated with the parameters that provided the best fits, at more wavelengths than used for building the grids in model space. Despite the high frequency discrepancies shown by the blue lines, the red lines show that the models reproduce well the spectral variation in the CH_3D feature (at 1.5552–1.5562 μm, Fig. 3).

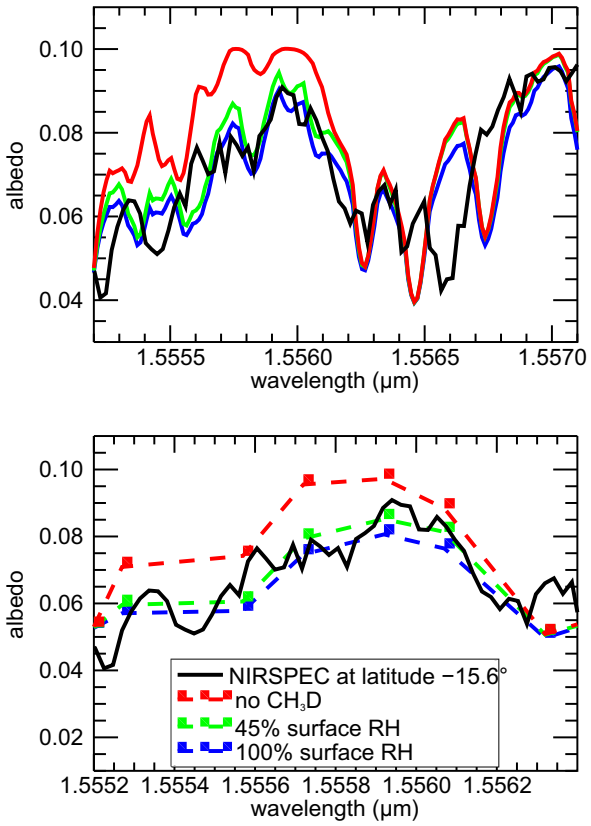

Fig. 3. Observation at 16°S latitude (black line), compared to models constructed for 45% (green), and 100% (blue) relative humidity at the surface. A model calculated assuming 45% CH_4 humidity and no CH_3D (red line) indicates the differing effects of CH_3D absorption and the poorly constrained CH_4 absorption. In the bottom plot the models were smoothed to a lower spectral resolution, to better indicate how spectra vary over the whole CH_3D feature, without the effects of the high resolution CH_4 structure. Only at 1.5552–1.5562 μm the effect of CH_3D is significant compared to CH_4.

indicator i_1, and 1.55527–1.55557 μm for indicator i_2, as shown in the first spectrum of Fig. 2. Fig. 4 presents the latitudinal variations of the three indicators, along with those of the best model fits. The indicators were chosen to maximize their different responses to changes in the methane abundance, haze scattering and surface albedo. As shown in Fig. 5, i_0 is the most sensitive to the methane abundance, while i_1 is saturated over most of the methane abundance range considered. Variations in surface albedo least affect i_1, which therefore indicates the scattering due to clouds and haze. Intermediate between i_0 and i_1, is i_2, which differentiates between changes in methane absorption and surface albedo. Fig. 6 displays the effect of methane variations on the indicators; we can see that i_0 is sensitive to the methane abundance in the lowest 10 km of Titan's atmosphere. Uncertainties in the CH_4 line parameters affect our results such that an error of 20% in CH_4 optical depths causes a change in the vertical contribution peak of 7% for i_0, 5% for i_2, and 0.5% for i_1.

Our initial model adopted the DISR haze parameters and Huygens GCMS methane profile, derived for 10°S latitude, which were adjusted to interpret spectra at other latitudes. We find that only three parameters need to be changed to reproduce the three indicators within their noise levels. The parameters are the methane abundance, the haze optical depth above 80 km and the surface albedo, which affect the three indicators as shown in Fig. 5. Model spectra were calculated in a uniform grid in the 3D space of these model parameters, and the fits were obtained from the combination that resulted in the best match on the 3D indicator space.

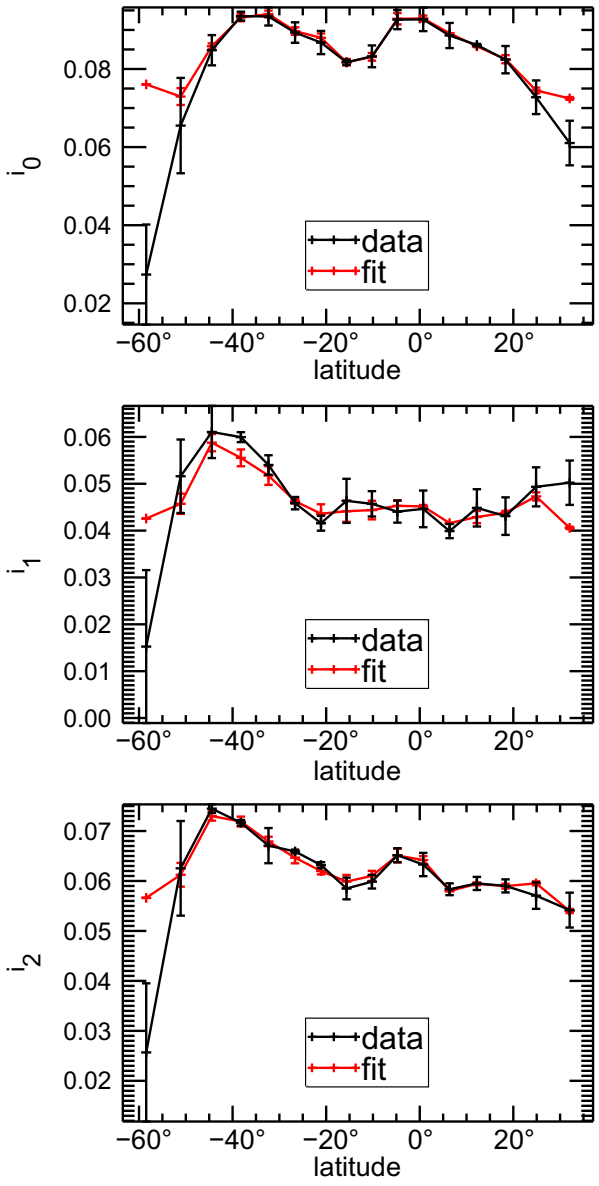

Fig. 4. Latitudinal variations of the three indicators, calculated for the data (black line) and model spectra (red line). The anomalies at the four endpoints (three to the south and one to the north) result from the proximity to the limb, which causes a large variation in geometry and optical depths within each spatial pixel. The uncertainties in the data indicators are derived from the variation within the three spectra that were averaged to make each one of the 16 spectra used.

4. Results

The results are shown in Fig. 7, along with the uncertainties that result from their derivation from the mean data indicators. The noise level and overlapping effects of the methane, haze and surface albedo prevent us from measuring relative methane variations smaller than 20%, as indicated by the high frequency oscillation and the average size of the errorbars in Fig. 7. Above this level, we find no change in methane abundance over the range 32°S–18°N. These uncertainties equivalently permit variations smaller than 10% for the humidity above the surface. The resulting 25^{+40}_{-15}% increase in the haze optical depth above 80 km from 10°S to the equator is consistent with that determined from analysis of VIMS data (Penteado et al., this issue). The derived surface albedos agree with the values determined for the same terrain using VIMS observations at 1.5567 μm. The ratio between highest and

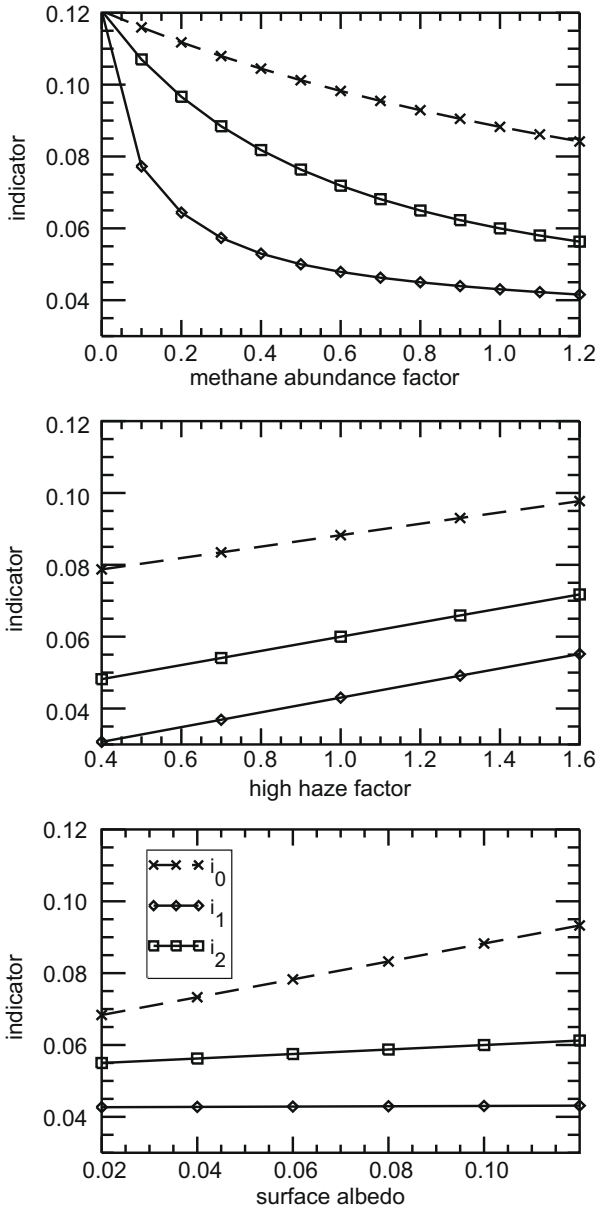

Fig. 5. Variation in the three indicators as a function of changes on the three model parameters. For each curve, the two model parameters not being varied were kept at their reference values (1.0 for methane abundance factor and high haze factor, 0.1 for surface albedo). These curves, along with Fig. 6, indicate that i_1 (solid line) is at a region of saturated methane absorption. Thus variations in i_1 mostly indicate variations in the haze.

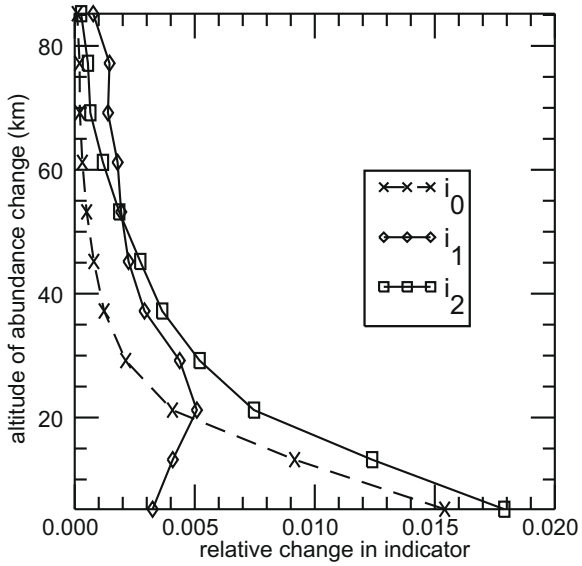

Fig. 6. Relative variation of the three indicators as a function of the altitude where the methane abundance is changed. The abundance is changed in a 5 km region by a multiplicative factor that is a linear function of altitude, from 0.5 at the indicated altitude, to 1 (no change) 2.5 km away. These profiles, along with Fig. 5, show that i_0 (dashed line) is most sensitive to the methane, i_1 (full line) is most sensitive to the haze, and i_2 (dotted line) is intermediary.

lowest surface albedos, $2.2^{+0.5}_{-0.3}$, is larger than the range found from the DISR observations at ~1.6 μm, of a different surface terrain (Keller et al., 2008).

Between 32°S and 51°S, the derived increase in haze optical depth, indicated by the sharp increase in Titan's albedo at 1.5552 μm (i_1, Fig. 4), suggests the presence of methane clouds on that region. Methane clouds typically observed south of 40°S (Roe et al., 2005a,b,2006; Griffith et al., 2005; Schaller et al., 2006a; Gendron et al., 2004; Gibbard et al., 2004; Bouchez and Brown, 2005) obscure the troposphere and are brighter than the surface. Thus clouds decrease the depths of methane absorption features. There is no independent constraint on the presence of clouds at the time of the observation, because there were no coinciding VIMS observations. Also the limited time available prevented us from recording lower resolution spectra, which would have revealed the cloud effects (as discussed in Griffith et al., 1998).

Our analysis demonstrates that high resolution ground-based data can measure methane abundance in the lower troposphere across Titan's disk. The $3\nu_2CH_3D$ lines probe the methane down to the surface, and thus complement lower resolution spectra (e.g. by Cassini VIMS) that measure the methane near the tropopause. Both the VIMS (Penteado et al., this issue) and Keck observations (discussed here) of the upper and lower troposphere, respectively, are consistent with a constant methane latitudinal profile from 32°S to 18°N. Yet, it is important to note that the derivation of the methane in the upper troposphere is strongly compromised by the uncertainties in the haze opacity, such that a drop as high as 60% in the methane abundance between 27°S and 19°N latitudes also agrees with the data (Penteado et al., this issue). The constant methane abundance in the lower troposphere is consistent with the atmosphere's thermodynamics, which indicates insufficient seasonal and daily variations in insolation to fuel large humidity changes (Griffith et al., 2008). The altitudes of the tropical clouds detected by Cassini VIMS measurements indicate, so far, that clouds reside at altitudes consistent with the methane abundance measured by Huygens (Griffith et al., 2009). Recent ground-based observations revealed a cloud that covers 5–7% of Titan's disk (Schaller et al., 2009). Yet the altitude evolution of this cloud was not determined; therefore it is unclear whether the cloud is deeply convective and whether it was triggered by an increase in humidity, resulting, for example, from cryovolcanism. We did not detect any local increase in methane that would indicate outgassing, yet we sampled, for lack of time, only a small fraction of Titan's disk. We have not yet investigated the humidity at high latitudes, where seasonal swings in insolation are sufficient to fuel large humidity changes (Griffith et al., 2008), and where lakes exist as a source of atmospheric methane. The high and apparently convective south polar clouds that were common near the summer solstice (until 2004) suggest the presence of more humid conditions than sampled in the tropics (Griffith et al., 2008). Future measurements of the methane abundance coupled with the temperature measurements by Cassini Radar occultations will

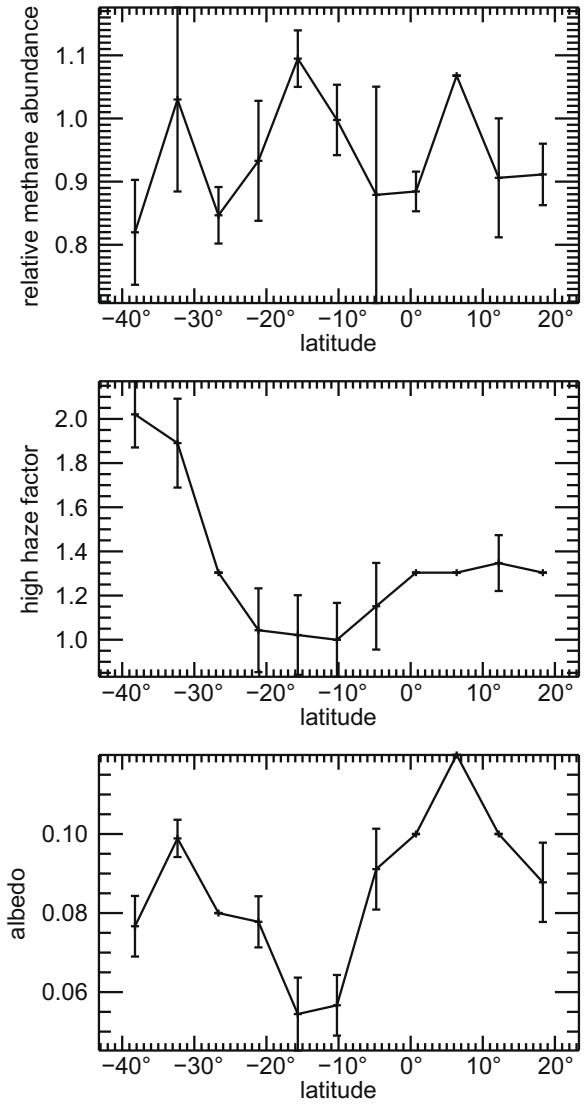

Fig. 7. The model parameters that resulted in the best fits to the data. These parameters are: the factor multiplying the Huygens GCMS methane profile (top), the factor multiplying the haze optical depth above 80 km (middle), and the surface albedo (bottom). The errorbars indicate the uncertainty originating only from the fit process (not including data noise): changes in the parameters within these ranges provide synthetic spectra within the variation present at each latitude bin.

indicate whether a more humid atmosphere at the poles leads to more convectively unstable conditions that would explain the observed high convective clouds.

Acknowledgments

The authors thank Christopher McKay for helpful discussions. The observations were in support of the Cassini–Huygens mission, during the NASA allocation for telescope observing time at the W.M. Keck Observatory. P. Penteado was sponsored by the Brazilian Government through CAPES. C. Griffith and P. Penteado were supported by the NASA Planetary Astronomy Program.

References

Barnes, J.W., and 34 colleagues, 2005. A 5-micron-bright spot on Titan: Evidence for surface diversity. Science 310, 92–95.

Barth, E.L., Rafkin, S.C.R., 2007. TRAMS: A new dynamic cloud model for Titan's methane clouds. Geophys. Res. Lett. 34, 3203. doi:10.1029/2006GL028652.

Bouchez, A.H., Brown, M.E., 2005. Statistics of Titan's south polar tropospheric clouds. Astrophys. J. 618, L53–L56.

Boussin, C., Lutz, B.L., de Bergh, C., Hamdouni, A., 1998. Line intensities and self-broadening coefficients for the $3\nu_2$ band of monodeuterated methane. J. Quant. Spectrosc. Radiat. Trans. 60, 501–514.

Boussin, C., Lutz, B.L., Hamdounia, A., de Bergh, C., 1999. Pressure broadening and shift coefficients for H_2, He and N_2 in the $3\nu_2$ band of $^{12}CH_3D$ retrieved by a multispectrum fitting technique. J. Quant. Spectrosc. Radiat. Trans. 63, 49–84.

Brown, M.E., Bouchez, A.H., Griffith, C.A., 2002. Direct detection of variable tropospheric clouds near Titan's south pole. Nature 420, 795–797.

Brown, M.E., Schaller, E.L., Roe, H.G., Chen, C., Roberts, J., Brown, R.H., Baines, K.H., Clark, R.N., 2009. Discovery of lake-effect clouds on Titan. Geophys. Res. Lett. 36, 1103. doi:10.1029/2008GL035964.

Brown, R.H., and 25 colleagues, 2006. Observations in the Saturn system during approach and orbital insertion, with Cassini's visual and infrared mapping spectrometer (VIMS). A&A 446, 707–716.

Brown, R.H., Soderblom, L.A., Soderblom, J.M., Clark, R.N., Jaumann, R., Barnes, J.W., Sotin, C., Buratti, B., Baines, K.H., Nicholson, P.D., 2008. The identification of liquid ethane in Titan's Ontario Lacus. Nature 454, 607–610.

Courtin, R., Gautier, D., McKay, C.P., 1995. Titan's thermal emission spectrum: Reanalysis of the Voyager infrared measurements. Icarus 114, 144–162.

Coustenis, A., Salama, A., Schulz, B., Ott, S., Lellouch, E., Encrenaz, T.H., Gautier, D., Feuchtgruber, H., 2003. Titan's atmosphere from ISO mid-infrared spectroscopy. Icarus 161, 383–403.

de Bergh, C., Chauville, J., Lutz, B.L., Owen, T., Brault, J., 1986. Monodeuterated methane in the outer Solar System II – Its detection on Uranus at 1.6 microns. Astrophys. J. 311, 501–510.

de Bergh, C., Lutz, B.L., Owen, T., Chauville, J., 1988. Monodeuterated methane in the outer Solar System III – Its abundance of Titan. Astrophys. J. 329, 951–955.

Gendron, E., and 13 colleagues, 2004. VLT/NACO adaptive optics imaging of Titan. A&A 417, L21–L24.

Gibbard, S.G., Macintosh, B., Gavel, D., Max, C.E., de Pater, I., Roe, H.G., Ghez, A.M., Young, E.F., McKay, C.P., 2004. Speckle imaging of Titan at 2 microns: Surface albedo, haze optical depth, and tropospheric clouds 1996–1998. Icarus 169, 429–439.

Griffith, C.A., Hall, J.L., Geballe, T.R., 2000. Detection of daily clouds on Titan. Science 290, 509–513.

Griffith, C.A., McKay, C.P., Ferri, F., 2008. Titan's tropical storms in an evolving atmosphere. Astrophys. J. 687, L41–L44.

Griffith, C.A., Owen, T., Miller, G.A., Geballe, T., 1998. Transient clouds in Titan's lower atmosphere. Nature 395, 575–578.

Griffith, C.A., and 26 colleagues. The evolution of Titan's Mid-latitude clouds. Science 310, 474–477.

Griffith, C.A., Penteado, P., Rodriguez, S., LeMouélic, S., Baines, K.H., Buratti, B., Clark, R., Nicholson, P., Jaumann, R., Sotin, C., 2009. Characterization of clouds in Titan's tropical atmosphere. Astrophys. J. 702, L105–L109.

Hirtzig, M., Coustenis, A., Lai, O., Emsellem, E., Pecontal-Rousset, A., Rannou, P., Negrão, A., Schmitt, B., 2005. Near-infrared study of Titan's resolved disk in spectro-imaging with CFHT/OASIS. Planet. Space Sci. 53, 535–556.

Keller, H.U., Grieger, B., Küppers, M., Schröder, S.E., Skorov, Y.V., Tomasko, M.G., 2008. The properties of Titan's surface at the Huygens landing site from DISR observations. Planet. Space Sci. 56, 728–752.

Lellouch, E., Coustenis, A., Gautier, D., Raulin, F., Dubouloz, N., Frere, C., 1989. Titan's atmosphere and hypothesized ocean – A reanalysis of the Voyager 1 radio-occultation and IRIS 7.7-micron data. Icarus 79, 328–349.

Lellouch, E., Coustenis, A., Maillard, J.-P., Strong, K., Deme, N., Griffith, C., Schmitt, B., 1992. The spectrum of Titan in the 1.06 and 1.28 micron windows. In: Kaldeich, B. (Ed.), Symposium on Titan. ESA Special Publication, vol. 338, pp. 353–358.

Lemmon, M.T., Smith, P.H., Lorenz, R.D., 2002. Methane abundance on Titan, measured by the space telescope imaging spectrograph. Icarus 160, 375–385.

Lopes, R.M.C., and 43 colleagues, 2007. Cryovolcanic features on Titan's surface as revealed by the Cassini Titan Radar Mapper. Icarus 186, 395–412.

Lorenz, R.D., and 14 colleagues, 2008. Fluvial channels on Titan: Initial Cassini RADAR observations. Planet. Space Sci. 56, 1132–1144.

Lutz, B.L., de Bergh, C., Maillard, J.P., 1983. Monodeuterated methane in the outer Solar System. I. Spectroscopic analysis of the bands at 1.55 and 1.95 microns. Astrophys. J. 273, 397–409.

McLean, I.S., and 14 colleagues, 1998. Design and development of NIRSPEC: A near-infrared echelle spectrograph for the Keck II telescope. In: Fowler, A.M. (Ed.), Society of Photo-Optical Instrumentation Engineers (SPIE) Conference Series. Society of Photo-Optical Instrumentation Engineers (SPIE) Conference Series, vol. 3354, pp. 566–578.

Mitchell, J.L., Pierrehumbert, R.T., Frierson, D.M.W., Caballero, R., 2006. The dynamics behind Titan's methane clouds. Proc. Natl. Acad. Sci., 18421–18426.

Niemann, H.B., and 17 colleagues, 2005. The abundances of constituents of Titan's atmosphere from the GCMS instrument on the Huygens probe. Nature 438, 779–784.

Orton, G., 1992. Ground-based observations of Titan's thermal spectrum. In: Kaldeich, B. (Ed.), Symposium on Titan. ESA Special Publication, vol. 338, pp. 81–85.

Penteado, P.F., Griffith, C.A., Greathouse, T.K., de Bergh, C., 2005. Measurements of CH_3D and CH_4 in Titan from infrared spectroscopy. Astrophys. J. 629, L53–L56.

Penteado, P.F., and 11 colleagues, this issue. Latitudinal variations in Titan's methane and haze from Cassini VIMS observations. Icarus. doi:10.1016/j.icarus.2009.11.003.

Porco, C.C., and 35 colleagues, 2005. Imaging of Titan from the Cassini spacecraft. Nature 434, 159–168.

Rannou, P., Montmessin, F., Hourdin, F., Lebonnois, S., 2006. The latitudinal distribution of clouds on Titan. Science 311, 201–205.
Roe, H.G., Bouchez, A.H., Trujillo, C.A., Schaller, E.L., Brown, M.E., 2005a. Discovery of temperate latitude clouds on Titan. Astrophys. J. 618, L49–L52.
Roe, H.G., Brown, M.E., Schaller, E.L., Bouchez, A.H., Trujillo, C.A., 2005b. Geographic control of Titan's mid-latitude clouds. Science 310, 477–479.
Roe, H.G., de Pater, I., Macintosh, B.A., McKay, C.P., 2002. Titan's clouds from Gemini and Keck adaptive optics imaging. Astrophys. J. 581, 1399–1406.
Samuelson, R.E., Nath, N.R., Borysow, A., 1997. Gaseous abundances and methane supersaturation in Titan's troposphere. Planet. Space Sci. 45, 959–980.
Schaller, E.L., Brown, M.E., Roe, H.G., Bouchez, A.H., 2006a. A large cloud outburst at Titan's south pole. Icarus 182, 224–229.
Schaller, E.L., Brown, M.E., Roe, H.G., Bouchez, A.H., Trujillo, C.A., 2006b. Dissipation of Titan's south polar clouds. Icarus 184, 517–523.
Schaller, E.L., Roe, H.G., Schneider, T., Brown, M.E., 2009. Storms in the tropics of Titan. Nature 460, 873–875.
Sotin, C., and 25 colleagues, 2005. Release of volatiles from a possible cryovolcano from near-infrared imaging of Titan. Nature 435, 786–789.
Stamnes, K., Tsay, S.-C., Jayaweera, K., Wiscombe, W., 1988. Numerically stable algorithm for discrete-ordinate-method radiative transfer in multiple scattering and emitting layered media. Appl. Opt. 27, 2502–2509.
Stofan, E.R., and 37 colleagues, 2007. The lakes of Titan. Nature 445, 61–64.
Tobie, G., Lunine, J.I., Sotin, C., 2006. Episodic outgassing as the origin of atmospheric methane on Titan. Nature 440, 61–64.
Tokano, T., McKay, C.P., Neubauer, F.M., Atreya, S.K., Ferri, F., Fulchignoni, M., Niemann, H.B., 2006. Methane drizzle on Titan. Nature 442, 432–435.
Tomasko, M.G., Doose, L., Engel, S., Dafoe, L.E., West, R., Lemmon, M., Karkoschka, E., See, C., 2008. A model of Titan's aerosols based on measurements made inside the atmosphere. Planet. Space Sci. 56, 669–707.
Turtle, E.P., Perry, J.E., McEwen, A.S., DelGenio, A.D., Barbara, J., West, R.A., Dawson, D.D., Porco, C.C., 2009. Cassini imaging of Titan's high-latitude lakes, clouds, and south-polar surface changes. Geophys. Res. Lett. 36, 2204. doi:10.1029/2008GL036186.
Yung, Y.L., Allen, M., Pinto, J.P., 1984. Photochemistry of the atmosphere of Titan – Comparison between model and observations. Astrophys. J. 55, 465–506.